

“PLASTIQUE” - A COMPUTER PROGRAM FOR 3D INELASTIC ANALYSIS OF MULTI-STOREY BUILDINGS

Vlasis K. Koumouisis, Eleni N. Chatzi and Savvas P. Triantafillou

*Institute of Structural Analysis and Aseismic Research
National Technical University of Athens
NTUA, Zografou Campus GR-15773, Athens, Greece
E-mail: vkoum@central.ntua.gr*

Abstract

The code “Plastique”, suitable for the inelastic dynamic analysis of R/C structures and its theoretical background are presented. Every structural entity is represented by a single nonlinear element through the implementation of a macro modeling approach. Three different types of 2D-macro elements are formulated namely; beams, columns and shear walls. The structural behavior of each element is evaluated using a flexibility formulation based on both element edge regions that follow a distributed plasticity law. A fiber model is used to define the monotonic strength envelope at each section. The hysteretic behavior of the structural elements is monitored by a smooth hysteretic model of Bouc-Wen type. This model is capable to express the stiffness degradation, strength deterioration and pinching phenomena which are observed in R/C elements under cyclic loading. Plane frames consisting of combinations of plane elements are linked at the levels of floors via diaphragms to assemble the 3D mathematical model of the structure. Solutions are obtained by direct integration of the equations of motion, while an iterative procedure is implemented to satisfy equilibrium at every time step. Finally, a damage analysis is performed using an appropriate damage model. The numerical examples presented herein reveal the features of the proposed analysis scheme.

Keywords: inelastic analysis, time history, Bouc-Wen, damage index

1 Introduction

A problem of major importance in structural engineering deals with the response of R/C structures subjected to dynamic loading. For load factored linear elastic analysis, suggested by the codes, the results are quite satisfactory, but do not reveal the characteristics of the true behaviour of the structure. However, if inelastic response is taken into account, more refined models are needed as to achieve a realistic behaviour. In recent years, significant research has been carried out in order to overcome the difficulties arising in such an analysis. Difficulties emanate not only from the inherent complexity of R/C structures, but also from the uncertainties related to terms such as dynamical loading, material nonlinearity and hysteresis.

Macro-modeling of structures has been one of the main methods introduced to simulate these complex phenomena. In macro-modeling simulation, the field of knowledge concerning the actual behaviour of reinforced concrete is incorporated in the structure using an element-based approach. In such a way, the well established, from matrix structural analysis, beam element is enriched with a moment curvature envelope describing the behaviour of both end sections, a hysteretic law and a relevant yield penetration rule for the beam. By introducing such an elasto-plastic element, one is able to simulate the gradual shift of the mechanical properties of the element as it passes from the elastic to the inelastic region of its response. The overall behaviour of the structure is assessed using a proper damage index.

An aspect of utmost importance, for a non linear analysis, is the hysteretic rule needed to model the cyclic response of the structure. Over the last twenty years, significant development has occurred in the so-called phenomenological approach of hysteresis. Beginning with Bouc's original formulation (1967, 1969, 1971) of the single degree degrading hysteresis model with pinching, many modifications have been subsequently introduced, such as the Bouc-Wen model (1976, 1980), the Baber-Noori model (1985, 1986) and the Reinhorn model (1996). These hysteresis models –also known as smooth hysteretic models- are capable of simulating a number of different types of loops using a single smooth hysteretic function affected by a set of user-defined parameters. In doing so, one can easily model the three main phenomena describing the cyclic response of R/C elements namely; stiffness degradation, strength deterioration and pinching behaviour due to bond-slip effects.

Following these rules, many computer programs have been developed, capable to perform a non-linear structural analysis such as DRAIN-2D (Kanaan and Powell,1973), SARCF (Chung et al.,1998; Gomez et al.,1990), IDARC (Park et al., 1978;Kunnath et al., 1992) and ANSR (Oughourlian and Powell,1982). The “*Plastique*” code presented herein, although maintains the elastoplastic behaviour within the 2D plane frames, works with a 3D stiffness of the entire structure based on diaphragmatic action.

2 Material Properties

Material properties are defined through certain conventional stress-strain curves both for unconfined concrete and reinforcing steel. In the former a parabolic stress-strain relationship with a softening branch is used, while in the latter a bilinear stress-strain diagram with hardening is implemented. The aforementioned stress – strain curves are depicted in Figure 1.

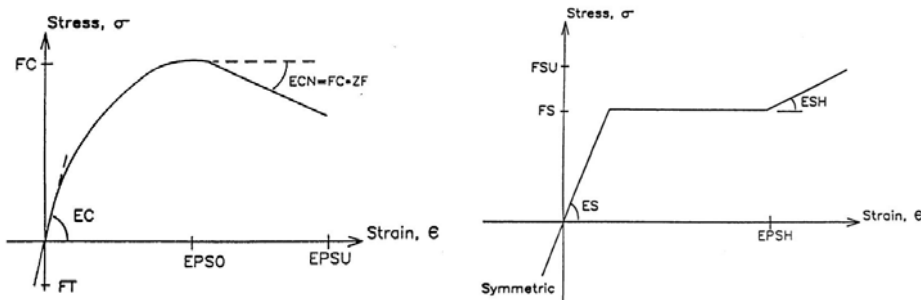


Figure 1. Stress –Strain diagrams a) for unconfined concrete and b) for reinforcing steel

3 Element Modeling

Three different types of two dimensional structural elements namely; beams, columns and shear walls are adequate to model the response of multi-storey buildings. By combining such elements one assembles multi-storey plane frames, which are linked together through diaphragms at the floor levels to create a 3D model of the structure.

3.1 Beam Element

Beam elements are considered as flexural elements with shear deformations with no axial deformations as beams belong to inextensional diaphragms and rigid zones at the ends to account for the stiffness increase at the joint, if needed. The element stiffness matrix varies throughout the analysis due to plasticity effects. In order to simulate such effects a hysteretic law and a spread plasticity model are introduced. The hysteretic model is formulated based on an initial moment-curvature relationship which represents the backbone skeleton curve. Such skeleton curves must be defined for each edge section of all elements. These curves can be either user defined or can be computed using a fiber

model and certain given properties of the section under consideration such as geometry, concrete and reinforcement properties.

3.2 Column Element

The column element formulation is identical to that of a beam, as columns are treated as 2D elements that participate separately to intersecting 2D frames. Plasticity zones are developed at the end regions of columns and axial deformations are taken into account.

3.3 Shear Wall Element

Shear wall elements are modelled combining an axial linear-elastic spring together with a nonlinear shear and a nonlinear flexural spring in series. In this case not only a moment-curvature skeleton curve is required, but a shear force-shear deformation curve as well, which are either user defined or computed through a fiber model.

4 Spread Plasticity Model

Inelastic deformations vary along element’s length. Consequently an element will also exhibit different flexibility characteristics. In order to formulate the elastoplastic flexibility matrix of such an element a spread plasticity model is introduced. This model can formulate an element’s flexibility matrix by taking into account the current stiffness (i.e. flexural stiffness concerning beams and columns and also shear stiffness for walls) at each end section, a corresponding yield penetration length and/or the elastic core stiffness depending on the values of the yield penetration lengths.

5 Yield Penetration Model

A yield penetration model is used to compute the yield penetration lengths at the end sections of an element as shown in Figure 2. Yield penetrations parameters α_A and α_B specify the portion of the element where the acting moment is greater than the corresponding yield moment of the section. For simplicity, a linear moment distribution is assumed even in the case of the presence of distributed loads. However one can subdivide each structural element into a number of elements in order to capture closely a parabolic variation.

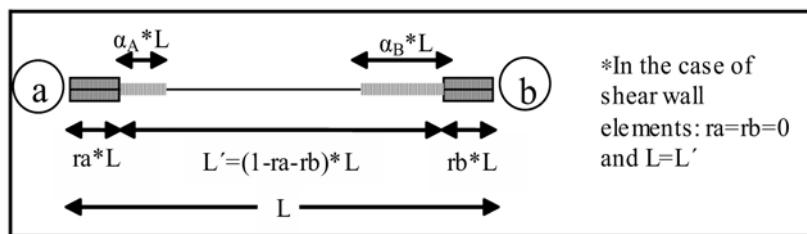


Figure 2. Yield Penetration Parameters

As long as the current moment distribution is defined, a set of geometrical oriented rules is used in order to define both the yield penetration lengths and the stiffness of the central part of the element. The yield penetration parameters are checked with the previous maximum penetration lengths, while the plastic regions of the element are considered only to expand and not to contract.

6 The Hysteretic Model

The smooth hysteretic model presented herein is a variation of the model originally proposed by Bouc (1967) and modified by several others (Wen 1976; Baber Noori 1985). The model was developed in the context of moment-curvature relationships of beam-columns. Therefore the stress variable is here

referred to as “moment” (M) and the strain variable as “curvature” (ϕ). In the case of shear-walls the hysteretic loop can be described in terms of a shear force-shear deformation relationship.

The use of such a hysteretic constitutive law is necessary for the effective simulation of the behavior of R/C structures under cyclic loading, since often structures that undergo inelastic deformations and cyclic behavior weaken and lose some of their stiffness and strength. Moreover, gaps tend to develop due to cracking causing the material to become discontinuous. The Bouc-Wen Hysteretic Model is capable of simulating stiffness degradation, strength deterioration and progressive pinching effects.

The model can be visualized as a linear and a nonlinear element in parallel, as shown in Figure 3. The relation between generalized moments and curvatures is given by:

$$M(t) = M_y \left[\alpha \frac{\phi(t)}{\phi_y} + (1 - \alpha) z(t) \right] \quad (1)$$

where M_y is the yield moment; ϕ_y is the yield curvature; α is the ratio of the post-yield to the initial elastic stiffness and $z(t)$ is the hysteretic component defined below.

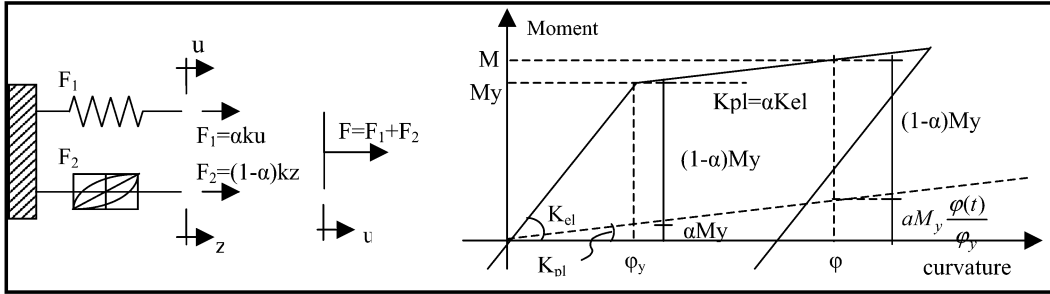


Figure 3. Bouc-Wen Hysteretic Model

The nondimensional hysteretic function $z(t)$ is the solution of the following non-linear differential equation:

$$\dot{z}(t) = f(\dot{\phi}(t), z(t)) \frac{1}{\phi_y} \text{ or alternatively } \frac{dz}{d\phi} = K_z \frac{1}{\phi_y} \text{ where } K_z = \left[A - B \frac{1 + \text{sign}(d\phi)}{2} \left(\frac{|z(t)| + z(t)}{2} \right)^{n_B} - C \frac{1 + \text{sign}(d\phi)}{2} \left(\frac{|z(t)| - z(t)}{2} \right)^{n_C} - D \frac{1 - \text{sign}(d\phi)}{2} \left(\frac{|z(t)| + z(t)}{2} \right)^{n_D} - E \frac{1 - \text{sign}(d\phi)}{2} \left(\frac{|z(t)| - z(t)}{2} \right)^{n_E} \right] \quad (2)$$

In the above expression A, B, C, D & E are constants which control the shape of the hysteretic loop for each direction of loading, while the exponents n_B , n_C , n_D & n_E govern the transition from the elastic to the plastic state. Small values of n_i lead to a smooth transition, however as n_i increases the transition becomes sharper tending to a perfectly bilinear behavior in the limit ($n \rightarrow \infty$).

The program defaults are:

$$A = 1, \quad C = D = 0 \quad \& \quad B = \frac{1}{b^{n_B}}, \quad E = \frac{1}{e^{n_E}} \quad \text{where } e = \frac{-M_y^-}{M_y^+}, \quad b = 1 \text{ and } n_B = n_E = n \quad (3)$$

The parameters C, D control the gradient of the hysteretic loop after unloading occurs. The assignment of null values for both, results to unloading stiffness equal to that of the elastic branch. Also, the model is capable of simulating non symmetrical yielding, so if the positive yield moment is regarded as a reference point, the resulting values for B and E are those presented in equation (3). The hysteretic parameter K_z is then limited in the range of 0 to 1, while the hysteretic function z varies from $-|M_y^- / M_y^+|$ to 1.

Finally, the flexural stiffness can be expressed as:

$$K = EI = \frac{dM}{d\phi} = M_y \left[\alpha \frac{1}{\phi_y} + (1-\alpha) \frac{dz}{d\phi} \right] = M_y \left[\alpha \frac{1}{\phi_y} + (1-\alpha) K_z \frac{1}{\phi_y} \right] = EI_0 [\alpha + (1-\alpha) K_z] \quad (4)$$

6.1 Hysteretic behavior Variations

a) Stiffness Degradation

The stiffness degradation that occurs due to cyclic loading is taken into account by introducing the parameter η into the differential equation:

$$\frac{dz}{d\phi} = \frac{K_z}{\eta} \frac{1}{\phi_y} \rightarrow K = EI_0 \left[\alpha + (1-\alpha) \frac{K_z}{\eta} \right] \text{ where } \eta = 1.0 + S_k \frac{\mu_{\max} + \mu}{2} \quad (5)$$

The parameter η depends on the current, $\mu = \phi / \phi_y$, and maximum achieved plasticity, $\mu_{\max} = \phi_{\max} / \phi_y$. S_k is a constant which controls the rate of stiffness decay. Common values for S_k are 0.1 and 0.05.

b) Strength Deterioration

The strength deterioration is simulated by multiplying the yield moment M_y with a degrading parameter S_β :

$$M(t) = S_\beta M_y \left[\alpha \frac{\phi(t)}{\phi_y} + (1-\alpha) z(t) \right] \quad (6)$$

The parameter S_β depends on the damage of the section which is quantified by the Damage Index DI:

$$S_\beta = 1 - S_d DI \text{ where } DI = \frac{\mu_{\max} - 1}{\mu_c - 1} \frac{1}{\left(1 - \frac{S_{p1} \int dE_{diss}}{4E_{mon}} \right)^{S_{p2}}} \quad (7)$$

In the above expression S_d , S_{p1} , S_{p2} are constants controlling the amount of strength deterioration; μ_c is the maximum plasticity that can be reached, $\mu_c = \phi_u / \phi_y$; $\int dE_{diss}$ is the energy dissipated before unloading occurs and finally E_{mon} is the amount of energy absorbed during a monotonic loading until failure as shown in **Figure 4**.

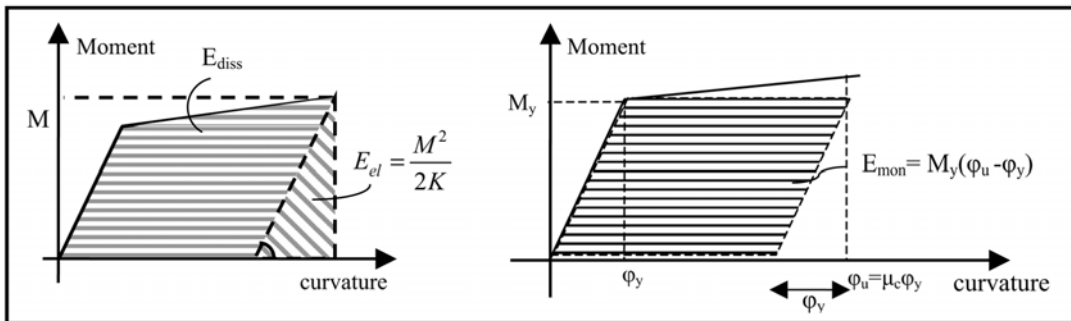


Figure 4. Dissipated Energy (Ediss) and Monotonic Energy (Emon).

c) Pinching or Slip

Pinching of hysteretic loops due to shear cracking and bond slip of the reinforcement is commonly observed in reinforced concrete structures during cyclic loading. This phenomenon is taken into account by introducing in the expression of K_z the “slip length” parameter a , and a function $f(z)$:

$$K_z^{pin} = \frac{K_z}{1 + a \cdot f(z) \cdot K_z} \tag{8}$$

In the above equation K_z^{pin} is the hysteretic parameter affected by pinching, K_z is the original expression of the hysteretic parameter obtained from (3) and parameters a , $f(z)$ are given by:

$$a = A_s(\mu' - 1) \quad \& \quad f(z) = \exp\left[-\frac{(z - z_m)^2}{z_s^2}\right] \tag{9}$$

where A_s is a control parameter which may be linked to the size of crack opening or reinforcement slip or both; μ' is the normalized curvature attained at the load reversal prior the current loading circle; z_s is the range where slip occurs. A non zero value of the parameter z_m will shift the effective slip region so that it is symmetric about $z = z_m$.

7 Method of Analysis

The computer program “*Plastique*” which is described herein, is capable to perform the different types of analysis, namely; Push-over analysis, Quasi-static analysis, Non-linear dynamic analysis and Eigenvalue analysis

The first two analysis types, although significantly simplified, can lead to valuable conclusions concerning the behavior of the structure and the possible collapse mechanism. The applied procedure can be described in brief as follows. In the case of 2-D analysis the structure is assumed to consist of a finite number of nodes interconnected by a finite number of elements. The types of elements have been described in section 3. In the case of 3-D analysis the structure is assumed to consist of the aforementioned 2-D frames, assuming a rigid diaphragm assemblage of their horizontal dof’s per floor slab. Loads may be applied at the nodes or along the elements. In both cases though, they are transformed to nodal loads.

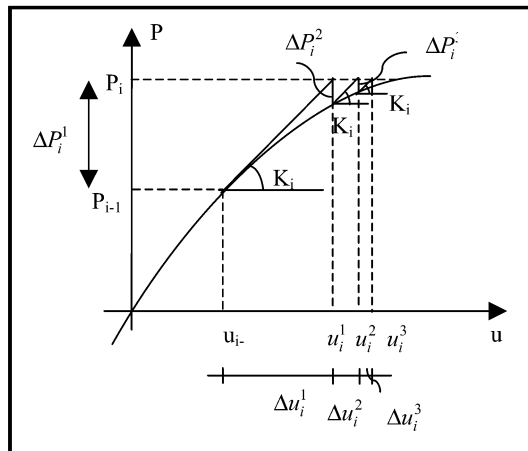


Figure 5. Modified Newton Raphson Method

After the formation of the stiffness matrix the equilibrium equations are solved by an efficient algorithm based on the Gaussian elimination method. The structure stiffness is stored in a banded form

to optimize the use of core storage and during arithmetic operations are avoided. An incremental method is applied for all types of analysis. The specified loads are divided to sufficiently smaller sub-loads, in order to simulate more efficiently the stress redistribution which occurs due to the non linear behaviour of the structure. An iterative process (modified Newton Raphson Method) is incorporated in each load step so that a higher level of accuracy can be achieved, as shown in Figure 5.

The member forces are computed for each load increment and the tangent stiffness matrix is updated to account for changes in any stiffness coefficient of the element. A spread plasticity model is used, as described in section 4, in order to simulate the changes in the flexibility in each element. In the case of the dynamic analysis the Newmark Method is used for the direct integration of the equations of motion.

The equation of motion to be solved at any stage of the analysis is written as:

$$[M]\{\ddot{U}\} + [C]\{\dot{U}\} + \{P_{int}\} = \{P_{ext}\} = -[M]\{S\}\{\ddot{U}_g\} \quad (10)$$

where [M] is the mass matrix; [C] is the damping matrix; [P_{int}] is the internal load vector of the structure; [P_{ext}] is the external load vector of the structure; [S] is a modal influence vector; [U] is the structure displacement vector and { \ddot{U}_g } is the ground acceleration vector.

The above system of equations is solved using the constant acceleration method, according to which equation (10) can be rewritten for time t+Δt and iteration k as:

$$[M]^{t+\Delta t} \cdot \{\ddot{U}\}^{(k)} + [C]^{t+\Delta t} \cdot \{\dot{U}\}^{(k)} + {}^{t+\Delta t} \{P_{int}\}^{(k-1)} + {}^t [K_t]^{t+\Delta t} \cdot \{\Delta U\}^{(k)} = {}^{t+\Delta t} \{P_{ext}\} \quad (11)$$

The hysteretic model applied is the Bouc Wen - Baber Noori model which, as mentioned previously, is able to simulate R/C behaviour such as stiffness degradation, strength deterioration and pinching. At every step of the analysis, the Damage Indices of the elements and the structure are calculated providing an evaluation not only of the inflicted damage, but also of the structure's residual strength and capacity to withstand further loading. The Damage Index for each section is given by relation (7). The Damage Index for each element is computed as the maximum Damage Index of its sections' and finally the Damage Index of the whole structure can be obtained from the following expressions:

$$DI = \sum_i \frac{E_{tot,i}}{\sum_i E_{tot,i}} (DI)_i \quad (12)$$

where (DI)_i is the Damage Index for each element and E_{tot,i} is the total amount of absorbed energy per element.

8 Numerical Examples

8.1 Example 1

This example demonstrates the usage of the different analysis and design options of “Plastique”. The structure used is a one bay single storey 2D frame shown in Figure 6.

A monotonic push-over analysis can provide the collapse mechanism of the particular structure as shown in Figure 7.

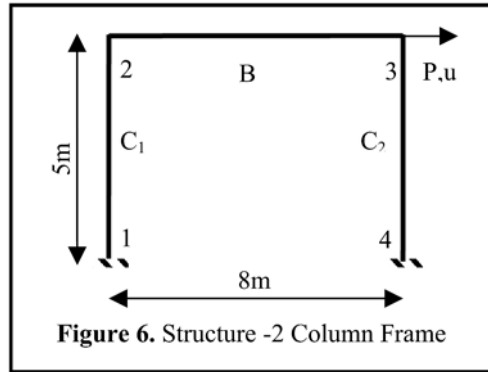


Figure 6. Structure -2 Column Frame

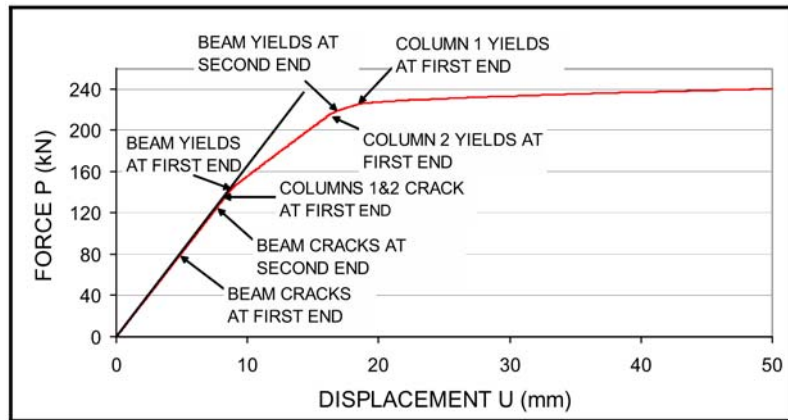


Figure 7. Possible Collapse Mechanism

In addition, a dynamic analysis is carried out. The accelerogram of the Northridge earthquake, normalized at 0.50g, was chosen for the particular analysis (Figure 8).

The resulting displacement time history, the force displacement hysteretic loop, as well as the final Damage Indices (DI) and yield penetration lengths are presented in the following figures (Figures 9 to 11).

In Figure 10, one can notice the gradual shift in the column section's stiffness due to stiffness and strength degradation effects, and the gradual shift of plastic deformation at a number of steps until the rest at a deformed state.

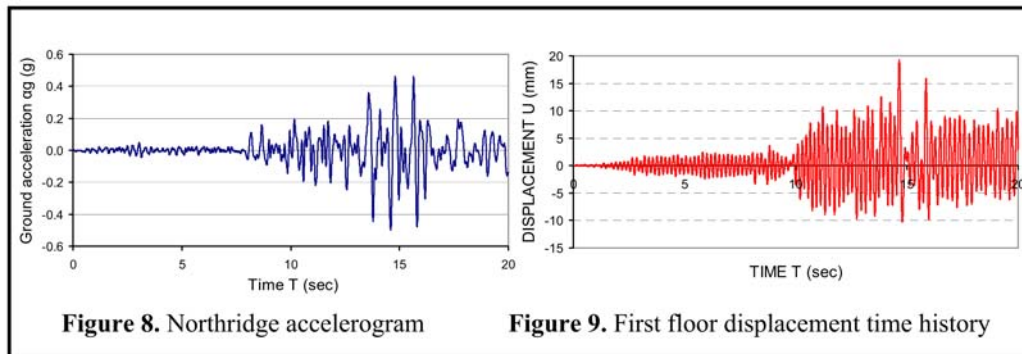


Figure 8. Northridge accelerogram

Figure 9. First floor displacement time history

The damaged state of the structure at the end of the analysis is depicted in Figure 11. The reduced sections are a graphical representation of the inelasticity distribution along each member's length. The damage index offers a measure of the accumulated damage at each member.

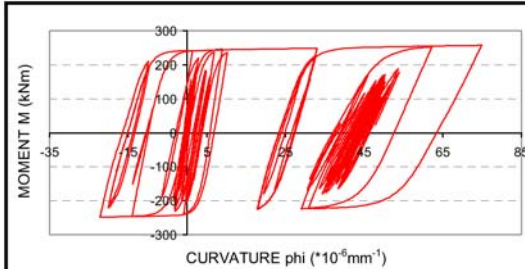


Figure 10. Moment-Curvature Hysteretic loop

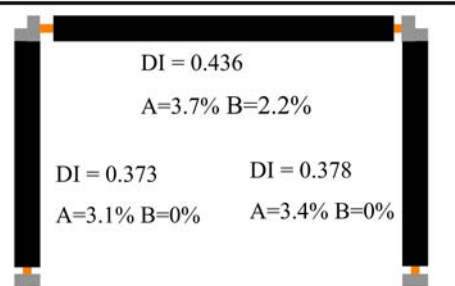


Figure 11. Final DI and yield penetration lengths

8.2 Example 2

As another example the behavior of a three storey building subjected to dynamical loading of time varying frequency content is presented. The Tabas (Iran – 0.68g) earthquake was chosen for this particular analysis and the method of wavelets was applied for the construction of the corresponding time-frequency spectrum. The analysis demonstrates the response of the structure to a short of “sliding” resonance between the first eigen frequency of the structure and the primary frequency of the excitation, that both are shifted as time progresses. The structure due to plastification and the excitation due to a time – frequency variation that often occurs in strong ground motion excitations.

The original Tabas accelerogram is presented in Figure 12 accompanied by its corresponding time-frequency spectrum (Figure 13).

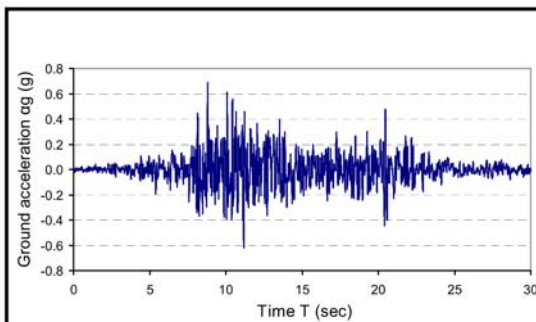


Figure 12. Tabas accelerogram

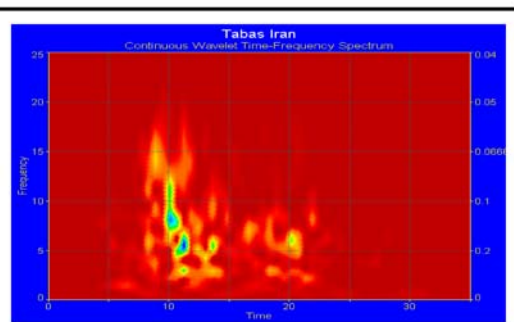


Figure 13. Time-Frequency spectrum

From the time-frequency spectrum one can identify the three peaks presented in Table 0. Since Max_2 and Max_3 have similar values and arise in relatively close time interval they can be substituted by an “equivalent” spectral frequency presented in the last row.

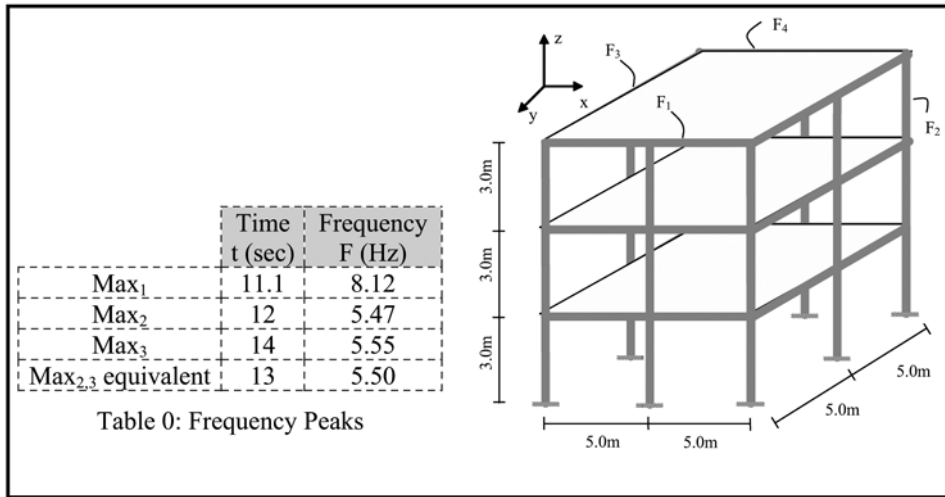


Figure 14. Three storey building

The 3D structure studied in the present example is depicted in Figure 14. A convenient set of geometrical/mechanical properties and hysteretic parameters was used in order to achieve an eigen frequency variation for the primary mode which would start from a value of 8.15Hz for a duration of 11.1 sec approaching 5.55 Hz around 13 sec. A dynamic analysis was performed using the Tabas accelerogram as excitation in the x direction. The structure's response is presented in Figure 15, where it can be observed that after $t = 13.5$ sec the top floor displacement increases rapidly, leading the structure finally to failure at $t = 14.4$ sec.

By careful examination of the results it turns out that most of the critical sections of the structural elements yield and fail within the time interval of 11 to 14.4 sec. Similar evidence is provided by examining the variation of the primary frequency of the building, that remains steady at approximately 8.15Hz for the first 12.5 sec, decreasing rapidly in steps due to the successive degradation phenomena to the value of 5.55Hz at around 13.5 sec (Figure 15).

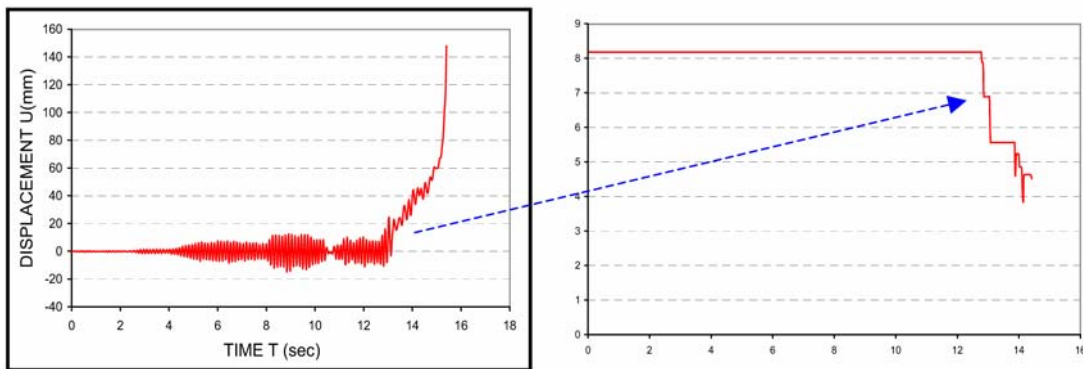


Figure 15. a) Top floor displacement time history- b) Frequency Variation.

In order to verify whether the failure is due to the previously described pattern of successive resonance a non linear analysis is performed on the previous structure after filtering out the second highest spectral frequency of the excitation (of approximately 5.552Hz), i.e by considering an excitation without the time – frequency variation. For this case although the structure suffers a severe damage does not collapse as it remains steady at a top storey displacement of the order of 50 mm (Figure 16).

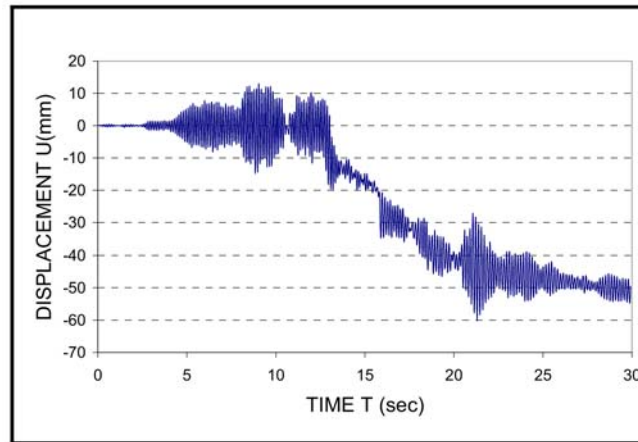


Figure 16. Top story displacement time history after filtering the accelerogram.

By examining the status of elements and its evolution in time a different development in the failure mechanism is observed mainly for $t > 13$ sec, which is due to the absence of the filtered frequency.

9 Conclusions

A new computer program, “*Plastique*”, for the inelastic analysis of structures is presented. A macro modeling approach is implemented, combined with a spread plasticity and a yield penetration model to account for the inelastic phenomena on structural response. By introducing a smooth Bouc Wen type hysteretic model a close to reality simulation of R/C cyclic response is achieved. An iterative procedure is used in order to solve the equilibrium equations. The program proves to be a versatile tool offering different analysis options. In comparison to other similar nonlinear analysis programs, “*Plastique*” is capable of performing a full 3D inelastic analysis, using the same model for every plan orientation of the seismic excitation.

Inelastic analysis reveals a more realistic response of the structure, demanding though a more accurate description of the structural properties and their variations. Seismic hazard analysis becomes even more crucial, as compared to an elastic analysis, while time-frequency distribution of the frequency content of an earthquake, as demonstrated in the second example, can be decisive on the fate of the structure.

References

- Klaus-Jürgen Bathe, “Finite Element Procedures”.
- E. N. Chatzi & S. P. Triantafillou. Diploma Thesis, (2004), «Inelastic analysis of multistory buildings with a Bouc-Wen type hysteretic model», NTUA.
- Anil K. Chopra, “Dynamics of Structures”, Prentice Hall Inc.
- Robert D. Cook, David S. Malkus, and Michael E. Plesha, “Concepts and applications of Finite Element Analysis”, Third Edition.
- S. Dobson, M. Noori, Z. Hou, M. Dimentberg, and T. Baber, (1997), “Modelling and random vibration analysis of SDOF systems with asymmetric hysteresis”.
- Sashi K. Kunnath, John B. Mander, and Lee Fang, (1996), “Parameter identification for degrading and pinched hysteretic structural concrete systems”.

- Young J. Park, Andrei M. Reinhorn, and Sashi K. Kunnath, (1987), "IDARC : Inelastic damage analysis of reinforced concrete frame – shear-wall structures", Technical Report NCEER-87-0008, State University of New York at Buffalo.
- J. S. Przemieniecki, "Theory of Matrix Structural Analysis".
- R. E. Valles, A. M. Reinhorn, S. K. Kunnath, C. Li, and A. Madan (1996), "IDARC 2D Version 4.0 : A Computer Program for the Inelastic Damage Analysis of Buildings", Technical Report NCEER-96-0010, State University of New York at Buffalo.